Journal of Scientific & Industrial Research
Vol. 85, July 2026, pp. 645-656
DOI: 10.56042/jsir.v85i7.28609

Experimental and Numerical Investigation of Perforation Pitch Effects on the Thermal–Hydraulic Performance of a Tubular Minijet Heat Exchanger

Shital Yashwant Waware[1,3]*, Ashok Mache[1,2]*, Sandeep Sadashiv Kore[2] & Anant Sidhappa Kurhade[3,4]

[1]Department of Mechanical Engineering, Vishwakarma Institute of Information Technology, Pune 411 048, Maharashtra, India

[2]Department of Mechanical Engineering, Vishwakarma Institute of Technology, Pune 411 037, Maharashtra, India

[3]Department of Mechanical Engineering, Dr. D. Y. Patil Institute of Technology, Sant Tukaram Nagar, Pimpri, Pune 411 018, Maharashtra, India

[4]Dnyaan Prasad Global University (DPGU), School of Technology and Research, Dr. D. Y. Patil Unitech Society, Sant Tukaram Nagar, Pimpri, Pune, 411 018, Maharashtra, India

Received 12 February 2026; revised 09 September 2026; accepted 15 September 2026

This study experimentally and numerically investigates the effect of perforation pitch on the thermal–hydraulic performance of a counter-flow tubular minijet heat exchanger. Three perforation pitches of 8, 10, and 12 mm were tested under the same operating conditions, with hot- and cold-water mass flow rates of 0.1154 and 0.0659 kg/s, respectively, and hot-water inlet temperatures of 55, 75, and 85°C. The Reynolds number (Re) was evaluated from the measured flow rate and hydraulic diameter, while a three-dimensional RANS $k-\varepsilon$CFD model was used to predict the flow and thermal characteristics. The experimental heat-transfer rates were 413.5 W, 963.7 W, and 908.7 W for the 8, 10, and 12 mm pitches, respectively. The 10 mm pitch therefore produced the highest heat-transfer rate, together with a cold-side outlet temperature of approximately 32.5°C and an effectiveness of 0.0625. The CFD predictions agreed closely with the experimental results, with deviations of approximately 1.5 – 1.6% for the three heat-transfer-rate comparisons. The 8 mm pitch generated higher turbulence but increased hydraulic resistance, whereas the 12 mm pitch reduced hydraulic resistance at the expense of weaker jet interaction and mixing. Thus, among the three investigated configurations, the 10 mm pitch provided the most favourable balance between heat-transfer enhancement and pressure-drop penalty.

Keywords: Convective heat transfer, Flow mixing, Perforation pitch, Pressure drop, Turbulence intensity

Introduction

Heat exchangers are engineering devices that transfer heat between fluids to conduct an efficient thermal exchange. Tubular heat exchangers offer simple and robust construction; however, they are also limited in low Reynolds numbers due to the development of boundary-layer. Passive methods, such as jet impingement and other techniques that improve turbulence and fluid mixing, can enhance heat transfer. Microscale impingement using minijets is an attractive and efficient method yet limited in its use for tubular heat exchangers. CFD provides the ability to analyze flow and temperature fields, in addition to providing an opportunity for optimization of key parameters, such as jet pitch wherein heat-transfer enhancement must be balanced against pressure loss.

Optimizing the pitch of perforation is essential for controlling turbulence intensity and breaking up low-velocity thermal boundary layers in minijet arrays, which governs the efficiency of heat transfer.[1] On the other hand, for counter-flow tubular geometry this increase is normally accompanied by increased hydraulic resistance, leaving no option but to trade between heightened convective mixing and the associated pressure drop.[2,3] The purpose of the study is to find the ideal distance between geometric shapes which ensures that heat transfer will be maximized, in addition to controlling set levels of power needed for pumping.[4,5] In addition, the comparative analysis will highlight how these pitch discrepancies affect flow topology and mixing performance to better understand the subtle interplay between geometric components on the total energy consumption of the system.[6,7] It targets that special hole distributions control the transition of laminar and turbulent regimes are required for creating a better cooling effect in high-thermal performance thermal management systems.[8,9] This systematic variation of these pitch parameters provides us with a fully featured basis for

*Authors for Correspondence
E-mail: shital.221p0009@viit.ac.in, ashok.mache@viit.ac.in

assessing the trade-off between beneficial cross-mixing of fluid and the associated loss in internal pressure.[10,11] The results elucidate the influence of the pitch ratio through investigation of Nusselt number (Nu) versus friction factor trade-off and indicate that this choice is key in balancing global thermal enhancement against dissipative hydraulic losses.[12] The empirical and predictive results provide guidance for the refinement of orientations that should be applied to enhance both geometric configurations of heat exchangers under practical operating constraints in terms of performance evaluation criterion.[13,14] In this manner, by identifying these empirical relations the paper tackles the complex interactions between jet-to-jet and space distribution of perforations.[15,16] To be specific, in this research we evaluate is the Nu optimized by configuring 8 mm, 10 mm or 12 mm while reducing friction factor penalty as incurred in high-density jet arrays.[17] This work employs a single performance metric to empirically quantify the compromise between heat transfer enhancement and the parasitic requirements for pumping power.[18] This study provides more detail about how the jet-to-jet spatial interaction affects the target wall and is, therefore, necessary in order to understand what low temperature flow structure and thermal gradients are created by each particular configuration. These investigations further delineate the development of vortex structures and their immediate influence on field synergy within the fluid domain.[19] Additionally, the evaluation also features an analysis of experimental results versus numerical predictions to guarantee accuracy in flow field predictions.[20] In doing so, the study lays out a solid predictive baseline against which future empirical measurements can be validated to disentangle many complex dependencies complicating orifice spacing and secondary flow development.[21] Such observations into secondary flow behaviors are paramount to refining the pitch-to-diameter ratio, which ultimately controls swirl intensity as well as the reduction in thermal resistance.[22] Several previous studies have shown that the local heat transfer is enhanced due to better flow mixing by minijet impingement at the surface, but an increase in heat transfer generally resulted in higher hydraulic resistance.[23]

Different investigators analysed the passive enhancers like twisted tapes, coil-wire inserts, fins and swirl generators in tubular heat exchangers. Swirling and turbulent flow are the methods to increase heat transfer, which causes significant pressure drop. Jet impingement heat transfer has been heavily investigated for flat plates and electronic cooling applications, which exploit the relatively high local heat transfer coefficients obtained due to stagnation point flow.

Most of the previous studies have focused on conventional tubular heat exchangers, surface modifications, inserts and common jet-impingement approaches. For example, the interplay between how perforation spacing affects flow mixing and turbulence generation, heat transfer enhancement, and pressure loss is still not fully determined. To fill this gap, the current research experimentally and numerically investigates three scenarios of perforation pitches (8, 10, and 12 mm) under the same operating conditions. The novelty of the study consists in evaluating both thermal performance and hydraulic behavior for these types of pitching configurations and in selecting the best configuration among all tested cases according to heat-transfer enhancement vs hydraulic resistance evaluation. The 10 mm pitch gives the maximum heat-transfer rate of 963.7 W and a corresponding effectiveness of 0.0625, thus representing the most favorable thermal–hydraulic performance of the three different configurations studied in this work.

The originality of this study is the systematic experimental and Computational Fluid Dynamics (CFD) investigation on perforation pitch (8, 10 and 12 mm) in a counter-flow tubular minijet HE. The effect of pitch on jet interaction, turbulence, heat transfer and hydraulic resistance is demonstrated by the study and the optimum configuration at a 10 mm pitch with optimal heat-transfer rate (963.7 W) which corresponds to an effectiveness of 0.0625 along with thermal-hydraulic performance balance ratio between heat-transfer enhancement versus pressure-drop penalty are established.

Tubular Minijet Heat Exchanger

The tubular type minijet heat exchanger considered here is one which is a compact counter-flow heat exchanger developed to augment the convective heat transfer by jet–induced flow mixing as shown in Fig. 1. The geometry is such that combines the benefits of classical tubular heat exchanges with localized jet impingement, thus providing superior thermal performance. The experiment that provides a description of the setup involves concentric-tube heat exchanger with hot and

cold water flowing through the tubes. The counter – flow configuration has been selected in order to achieve a maximum, effective temperature which increases the heat transfer efficiency. Copper is a material that has good thermal conductivity and corrosion resistance and can be used as an inner tubing for transferring heat. The inner tube has an internal diameter of 11 mm and a wall thickness of 2 mm, and effective heat transfer length to the fluid is 281 mm. These were made small, but just with enough surface area to transfer heat exchanges.

Blast impingement is accomplished through the tubular heat exchanger by placing a number of ported minijets along the path. The cold water travels up past the outside of the inner tube where heat is drawn through the wall of that tube. The entire test section is provided with insulation to reduce heat losses to the environment, so that only heat transfer between both fluid streams takes place. In general, tubular minijet heat exchanger design provides a substantial enhancement of heat transfer with acceptable pressure drop and can be used for compact Heat Exchanger applications such as electronic cooling, process heat recovery and thermal management systems.

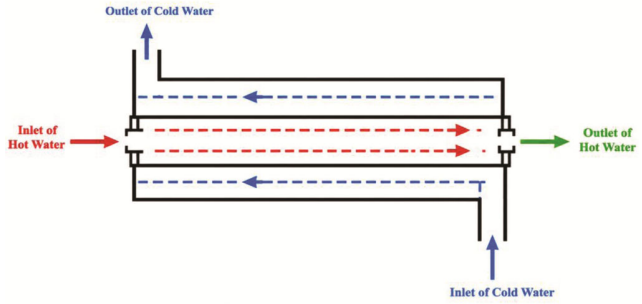

Fig. 1 — Counter-flow tubular mini-jet heat exchanger

Experimental Methodology

Experimental Setup

A test rig was designed and as shown in Fig. 2. The facility involves a hot water loop, cold water loop and two measuring systems with the mounted test section counter flow. The hot fluid reservoir was a 50 L commercially available hot water storage tank made of mild steel. Immersion heater 2 KW electric hot water immersion heater in vessel complete with temperature control for hot-water inlet. The hot water was pumped through the internal tube of the heat exchanger using a small magnetic pump to keep flow rates constant. Cold water was circulated in counter-current through the annular space of the heat exchanger. The hot and the cold-water line were provided with a rotameter (HQ series) to measure precisely the mass flow rate, (Kg/h). For each test the

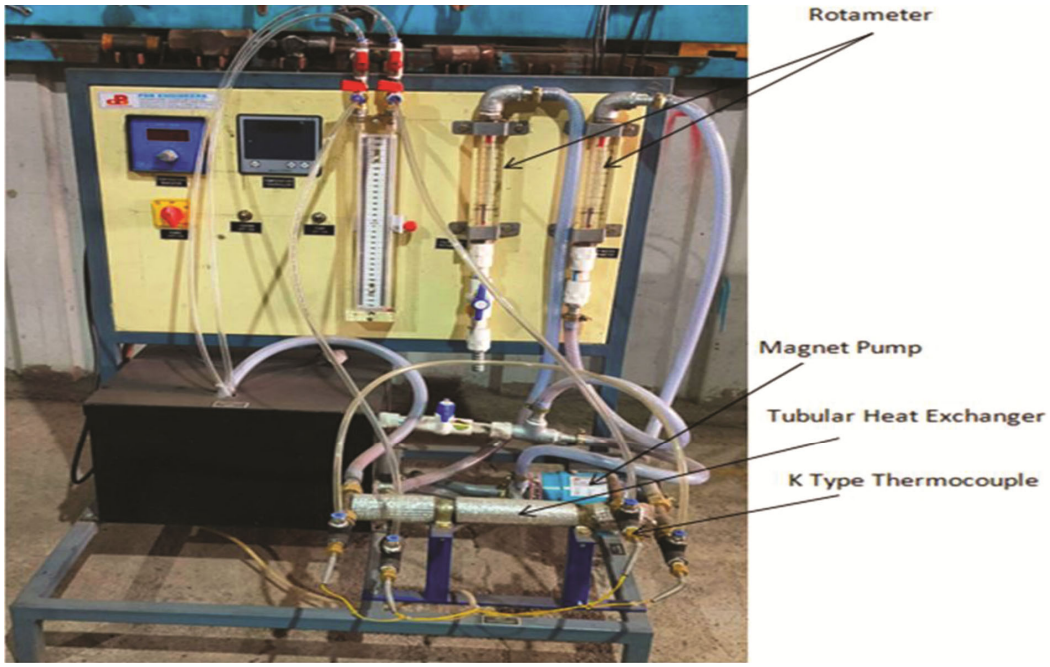

Fig. 2 — Experimental setup showing rotameter, magnetic pump, thermocouples, and tubular heat exchanger

flow rates for both fluids varied in increments from 1 Through 15 LPM as permitted.

Both hot and cold fluid streams were monitored by means of K-type thermocouples; one at the inlet orifice side and other at outlet orifice side in both hot as well as cold sides. Real-time temperature measurement was obtained using a digital temperature indicator. Pressure loss in the inner tube was also measured by U-tube manometer to determine frictional losses at different flow rates.

The tests were performed for hot (inlet preheated) water inlet temperatures of 55°C, 75°C and 85°C; while the cold-water inlet temperature was kept nearly constant. High heat transfer coefficient, Nu and pressure drop experiments were conducted for different mass flow rates at all inlet temperatures. The system was equilibrated before sampling of the experimental points.

Experimental Uncertainty Analysis

To quantify the uncertainty in the experimental results, it was done by combining all uncertainties of each parameter involved (in fluid temperature and mass flow rate and pressure-drop measurements). Two K-type thermocouples were used to measure the hot-water and cold-water temperatures; rotameters were applied for measuring the flow rates of each fluid, a U-tube manometer was employed to measure the pressure drop. To derive the uncertainty in calculated heat-transfer parameters, each measurement uncertainty was propagated through the written calculation equations. The Measurement and Propagated Uncertainty has explained in Table 1.

For a calculated parameter $\boldsymbol{R = f(x_1, x_2, \ldots, x_n)}$, the combined uncertainty was estimated using the root-sum-square method,

$$\mathbf{U_R} = \sqrt{\left(\frac{\partial R}{\partial x_1}\mathbf{U_{x1}}\right)^2 + \left(\frac{\partial R}{\partial x_2}\mathbf{U_{x2}}\right)^2 + \cdots + \left(\frac{\partial R}{\partial x_n}\mathbf{U_{xn}}\right)^2} \quad \ldots (1)$$

where, $\boldsymbol{U_R}$ = combined uncertainty in the calculated parameter and $\boldsymbol{U_{x_i}}$= the uncertainty associated with each measured variable.

An additional check of the experimental reliability was performed from the energy balance between hot and cold streams. Data with an energy-balance difference of < ±5% were also accepted as experimental values. The experiments were also validated against CFD results with a good agreement of about ±2–5%, which further supports the reliability of the measurements.

Results and Discussion

The thermohydraulic behaviour of the tubular minijet reactor can be fully studied also over an extended range of operating conditions. The objectives of the experiments were to study effects mass flow rate, hot water inlet temperature, Re and minijet-induced flow disturbance on heat transfer coefficient, Nusselt number, pressure drop as well as friction factor as significant performance parameters.

Effect of Reynolds Number on Nusselt Number

The convective heat transfer enhancement effect of the minijet configuration was quantified, based on Reynolds and Nusselt numbers. The experimental values further indicate that Re and Nu are linearly related for all operation conditions.

The relationship between Re and Nu clearly demonstrates enhanced convective heat transfer due to the minijet configuration explained in Fig. 3. Experimental observations show an almost linear rise in Nu with increasing Re across all operating

Table 1 — Experimental measurement and propagated uncertainty

Measured / Calculated parameter	Measurement range	Instrument / Method	Uncertainty
Hot-water temperature, Th	55–85°C	K-type thermocouple	±0.5°C
Cold-water temperature, Tc	≈29°C	K-type thermocouple	±0.5°C
Mass flow rate Hot water, ṁh	0.1154 kg/s	Rotameter	±2.0%
Mass flow rate Cold-water, ṁc	0.0659 kg/s	Rotameter	±2.0%
Pressure drop, ΔP	300–3000 Pa	U-tube manometer	±1.0%
Tube diameter, D	11 mm	Dimensional measurement	±0.1 mm
Heat-transfer rate, Q	413.5–963.7 W	Calculated	±3.0%
Reynolds number, Re	2000–16000	Calculated	±2.5%
Nusselt number, Nu	—	Calculated	±3.5%
Convective heat-transfer coefficient, h	—	Calculated	±3.5%
Friction factor, f	—	Calculated	±3.0%

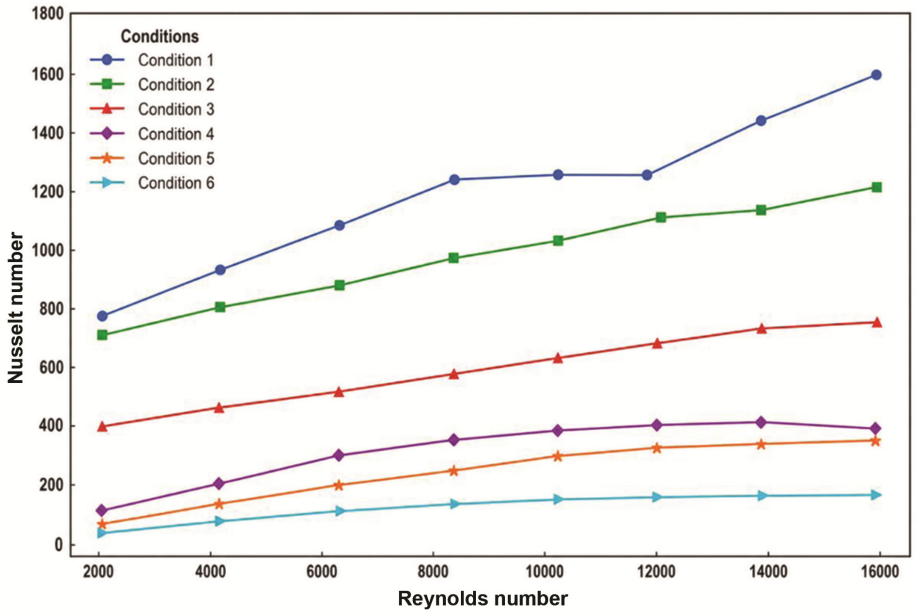

Fig. 3 — Comparison of Nusselt number enhancement with Reynolds number for different mini-jet operating conditions

conditions, confirming the strong dependence of heat transfer on flow intensity. Even at low Re numbers, where the flow is clearly in a transition phase, group of minijets mixes with main flow and provides local turbulence and in turn high Nu in comparison to smooth tube Heat Exchangers. With a further rise in Re, the synergistic enhancement of bulk flow turbulence and jet impingement in the hydrodynamic entrance region heavily intensifies heat transfer. Under HW inlet temperature of 55°C, the ranges for Nu enhancement are from 393 to 797, and they follow similar trend at 75 and 85°C. Among the six operating conditions, C1 consistently has highest Nu numbers leading least resistant heat transfer; especially that is true in C6. The distinct gap between the curve attributes to the effect of operation conditions, i.e., higher S ratios facilitate a more violent movement of turbulence and fluid mixture. In general, the findings validate Re as a primary controlling parameter for convective heat transfer, with its impact vastly enhanced by minijet-induced flow disturbances.

Pressure Drop Characteristics

The pressure drop behaviour demonstrates that increases with increasing hot water mass flow rate and inlet temperature shown in Fig. 4. With the increasing mass flow rate these Re will be higher and the convective heat transfer velocity increases as well as the improved intensity of turbulence, by jet

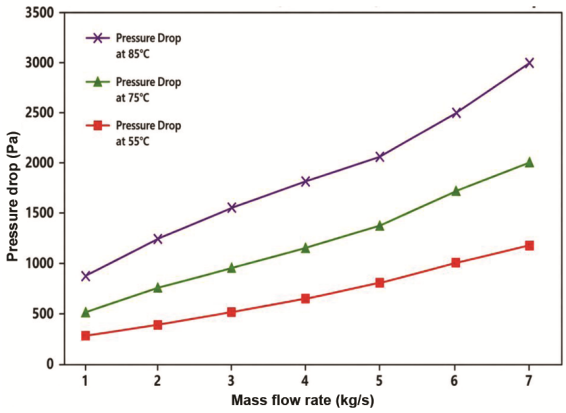

Fig. 4 — Effect of hot water mass flow rate on pressure drop at different inlet temperatures

impingement inside to heat exchanger. There are also the extra pressure losses due to flow separation and reattachment in the vicinity of the jet interaction regions, enhancing momentum dissipation. The results indicate that the highest-pressure drop is at 85°C, followed by 75°C and 55°C because of the interaction between flow rate and fluid. While the pressure loss increases with the increased turbulence and heat transfer, measured values still lie within an acceptable range for compact heat exchangers. This means that the improved heat transfer due to minijet-induced flow impingement also comes with a relatively low pumping penalty.

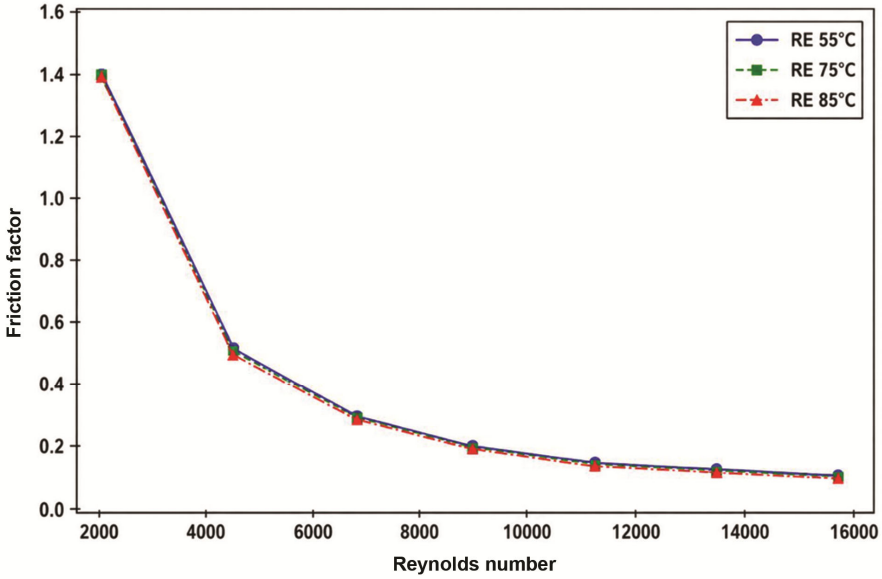

Fig. 5 — Effect of Reynolds number on friction factor at different fluid temperatures

Friction Factor Variation

The friction factor-Re correlation reflects the hydraulic behaviour of minijet heat exchanger with gases at different fluid temperatures explained in Fig. 5. It is found that the friction factor behaves monotonically with respect to Reynolds number, which is consistent with the traditional internal flow. At lower Reynolds numbers higher friction factor values are observed due to the domination of the viscous effects and less mixing in the flow. Whereas, as Re increases the inertia effects are dominant and minijet turbulence leads to slower transition from laminar flow, thus better energy dissipation and lower friction factor. The trends intersect the longer they lie, which makes sense, since temperature effects only slightly compared to the Reynolds number. Overall, it is demonstrated that the minijet arrangement significantly enhances heat transfer with very minor hydraulic drawback and would thus be very attractive for compact heat exchanger applications.

Thermal–Hydraulic Performance Assessment

The variation of the convective heat transfer coefficient with the Re indicates that minijet heat exchanger would offer a good thermal–hydraulic performance explained in Fig. 6. With the increase of Reynolds number, heat transfer coefficient increasing the laws of all operating conditions were all "monotone type", but the larger amplitudes, with the flow in impetus and Turbulence intensity and grow

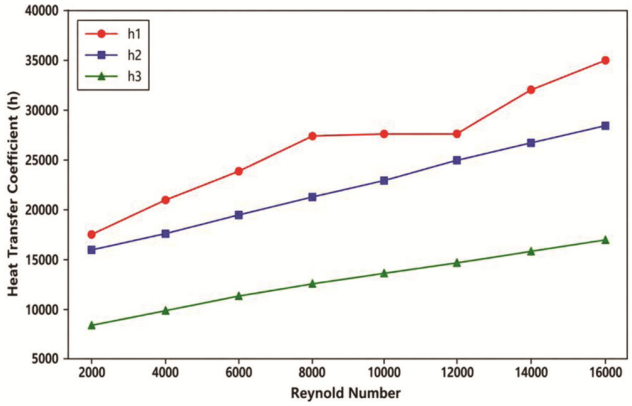

Fig. 6 — Effect of Reynolds number on convective heat transfer coefficient

convective heat transfer. The use of minijet injection is effective in breaking up the thermal boundary layer and permits much higher local rates of heat transfer than possible with conventional tube arrangements. Although the rise of Re number results in an enhanced fanning friction factor and pressure drop, the increment of heat transfer coefficient and Nu is much greater than hydraulic penalty. Such a balance reveals that the trade-off of hydraulic loss with respect to good thermal performance is yet acceptable. The results reveal that minijet–cantered designs offer an effective solution for generating compact and high-performance heat exchanger systems having appealing thermal–hydraulic qualities.

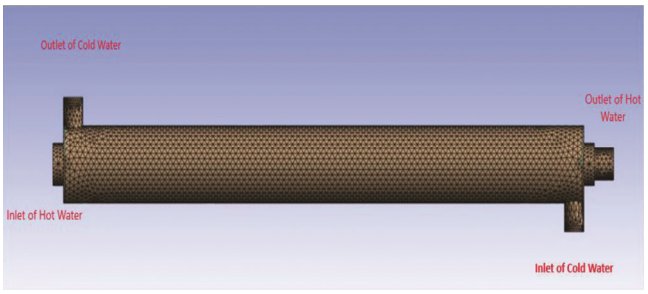

Fig. 7 — Computational mesh and boundary conditions of the tubular mini-jet heat exchanger

Numerical Investigation (CFD)

Geometry and Mesh Generation

A 3D geometrical model of the tubular minijet heat exchanger was generated by commercial CAD software and brought into ANSYS Fluent for simulations. The geometry faithfully reproduces the experimental test column and inner tube, outer tube and minijet feature associated with flow impingement/turbulence generation as explained in Fig. 7.

The computational domain is composed of a hot water inner pipe and the heat exchanger structure (inner shell). The cold water is passed through annular passage formed between the inner pipe and the outer shell. Furthermore, the model has numerous minijet holes and fluid jets passing through same for impingement against the inner tube surface for increased mixing and heat transfer between the same. A structured hexahedral-element mesh was created to guarantee numerical stability and better exactness of solution. Emphasis was placed upon mesh refinement close to walls and jet impingement locations, where significant velocity and temperature gradients are anticipated. To correctly consider nearwall effects, boundary layer inflation was implemented with several prism layers on solid walls to capture the viscous sublayer. The final mesh included 1,731,884 control volume cells determined using a mesh independence study which shows, there were less than ±2% changes in the Nu and pressure drop as the number of cells increased. This mesh resolution was determined to yield a best compromise between numerical error and computer time.

To guarantee the mesh independence of the numerical results, a grid-independence study was conducted. The mesh was gradually refined, especially around the minijet openings, impingement zones and solid walls. The monitoring parameters are chosen to be the Nu and pressure drop values as they are most affected by the velocity and thermal gradients resolution. The final mesh 1,731,884 cells was chosen for the simulations as any further refinement of the mesh produced changes in Nu and pressure drop of less than ±2%. This criterion was deemed sufficient to balance numerical accuracy and costs.

CFD Boundary Conditions and Numerical Settings

The CFD simulations were conducted in an ANSYS Fluent environment using a three-dimensional, steady-state incompressible flow model. The inlet boundary condition with mass-flow hot and cold-water streams specified as in the experiments (0.1154 kg/s for hot water stream + 0.0659 kg/s for cold one). Hot-water inlet temperature of 55, 75 and 85°C were adopted in the simulations, while cold-water inlet temperature was set at its experimental condition. At both fluid outlets, pressure-outlet conditions were used. The fluid–solid interfaces were modelled as two-sided thermal walls, while the external surfaces are treated as adiabatic, which simulates the insulated experimental test section.

The structure was fully hexahedral with reduced local refinement around the minijet openings, impingement regions and solid walls. To solve the near-wall velocity and temperature gradients, as well as to capture the viscous sublayer appropriately viscous effect was introduces into along with prism layer. This resulted in a final computational mesh with 1,731,884 cells. A mesh-independence investigation indicated that Nu and pressure drop with finer mesh refinement did not vary by more than ±2%.

The flow was modelled with Reynolds-averaged Navier–Stokes (RANS) and standard k – ε turbulence model was chosen to simulate the jet-induced turbulent internal flow. The stability of residuals in the governing equations as well as minimal change in monitored heat-transfer rate, outlet temperatures and

pressure drop with sustained further iterations indicated convergence. Then, the numerical results were compared against the experimental measurements and revealed ±2–5% mismatch in data indicating the significance of CFD methodology.

Governing Equations and Turbulence Modelling

It is taken for granted that the flow and heat transfer in the minijet heat exchanger tubular was three— dimensional, steady state, incompressible and turbulent. These equations were discretized by the Finite Volume Method (FVM).

Continuity Equation

$$\nabla.(\rho \mathbf{V}) = 0 \quad \ldots (2)$$

where, ρ= fluid density (kg/m³), $\mathbf{V}$ = velocity vector (m/s), $\nabla \cdot$ = divergence operator, representing the net mass flow per unit volume.

Momentum Equation

$$\nabla.(\rho \mathbf{V}\mathbf{V}) = -\nabla_p + \nabla.[\mu\text{eff}\,(\nabla \mathbf{V} + \nabla \mathbf{V}^T)] \quad \ldots (3)$$

where, p = static pressure (Pa), μ_{eff} = effective dynamic viscosity (Pa·s), $\nabla \mathbf{V}$ = velocity-gradient tensor, $\nabla \mathbf{V}^T$ = transpose of the velocity-gradient tensor, ∇p = pressure-gradient vector (Pa/m).

Energy Equation

$$\nabla.\left(\rho C_p \mathbf{V}T\right) = \nabla.[\text{keff}\,(\nabla T)] \quad \ldots (4)$$

where, k_{eff} = effective thermal conductivity (W/m·K), ∇T = temperature gradient (K/m).

Turbulent Kinetic Energy Equation

$$\nabla.(\rho \mathbf{V}k) = \nabla.\left[\left(\mu + \frac{\mu_t}{\sigma k}\right)\nabla k\right] + G_k - \rho\varepsilon \quad \ldots (5)$$

where, k = turbulent kinetic energy (m²/s²), μ_t= turbulent viscosity (Pa·s), σ_k= turbulent Prandtl number for turbulent kinetic energy, G_k= production rate of turbulent kinetic energy, ε = turbulent kinetic-energy dissipation rate (m²/s³).

The continuity equation represents the principle of mass conservation within the flow domain. It ensures that the mass flow rate remains constant, implying that there is no accumulation or loss of mass inside the control volume. This equation for isochoric flow assures that the velocity field fulfils the condition of being divergence-free for incompressible flow, a property needed when predicting internal fluid flows accurately.

The energy equation corresponds to this amount of heat that is conserved for the flow field. It includes heat transfer by convection of the fluid movement and heat conduction through thermal diffusion. The left-hand side denotes the convective energy transport due to the movement of fluid, while the right-hand side indicates heat conduction dominated by k_{eff}, an effective thermal conductivity that accounts for both molecular and turbulence contributions. This equation is indispensable in predicting the temperature field and evaluating convective heat transfer characteristics inside of turbulent flow channels.

The turbulence effects were simulated by using Reynold-Averaged Navier—Stokes (RANS) methodology with a standard k–ε turbulence model which is stable, fast to calculate and suitable for disturbances in jet-induced internal turbulence. Turbulent kinetic energy (k) and dissipation rate (ε) transport equations were resolved to very well predict the turbulence intensity and the eddy viscosity in the flow domain.

CFD Model Validation

Comparison of CFD predictions and experimental results under simulated operating conditions from the restriction rake test, it is expected that the numerical model accuracy was evaluated upon comparison with measurements. Hot and cold outlet temperatures and heat transfer have been selected as key performance parameters for the validation. The percentage discrepancy between experimental and CFD values was determined by,

$$\text{Error}\,(\%) = \left|\frac{X_{CFD} - X_{EXP}}{X_{EXP}}\right| \times 100 \quad \ldots (6)$$

where, X_{CFD} = the numerical prediction and X_{Exp} = the corresponding experimental measurement. Heat-transfer rate and outlet temperature were used as the primary validation parameters. A lower percentage error indicates closer agreement between the experimental and numerical results.

Comparison of Experimental and CFD Results for Different Perforation Pitches is given in Table 2. This ensures that the employed numerical model, mesh generation, and boundary conditions can accurately predict the thermo-hydraulic performance of the tubular minijet heat exchanger.

CFD based Interpretation for Pitch Optimization

The CFD predictions for the 8 mm pitch perforation configuration are characterized by high

turbulence intensity, because of tightly packed perforations, increasing fluid mixing inside the exchanger. The flow distribution becomes uneven in some areas which introduces localized perturbations. The tight distribution of the perforations generates also a rise in hydraulic resistance that corresponds to greater pressure losses. As such, even when strong turbulence and transport constraints are present the overall heat transfer performance remains only moderate.

Table 2 — Comparison of experimental and CFD results for different perforation pitches

Pitch (mm)	Parameter	Experimental	CFD	Relative error (%)
8	Heat transfer rate (W)	413.5	420.2	1.6
10	Heat transfer rate (W)	963.7	978.5	1.5
12	Heat transfer rate (W)	908.7	922.1	1.5
10	Hot-side outlet temperature (°C)	83.0	83.6	0.7

In pitch optimization studies, this configuration represents the high-turbulence, high-resistance limit. When compared with medium pitch (10 mm), the CFD results suggest that excessive disturbance does not proportionally increase useful heat transfer.

CFD Analysis of 8 mm Pitch Configuration

CFD study of the 8 mm pitch configuration reveals that jet perforations located close together create ample interaction, mixing and turbulence when injected, effectively disrupting the thermal boundary layer as explained in Fig. 8(a). We observe from the contour of temperature that heat continuously transfers from hot water entering at around 85°C to cold water entering at around 29°C; indeed, high turbulence improves convective thermal transfer, but closely spaced jets also lead to greater flow resistance and pressure losses, which restricts further thermal improvement. The experimental heat-transfer rate is

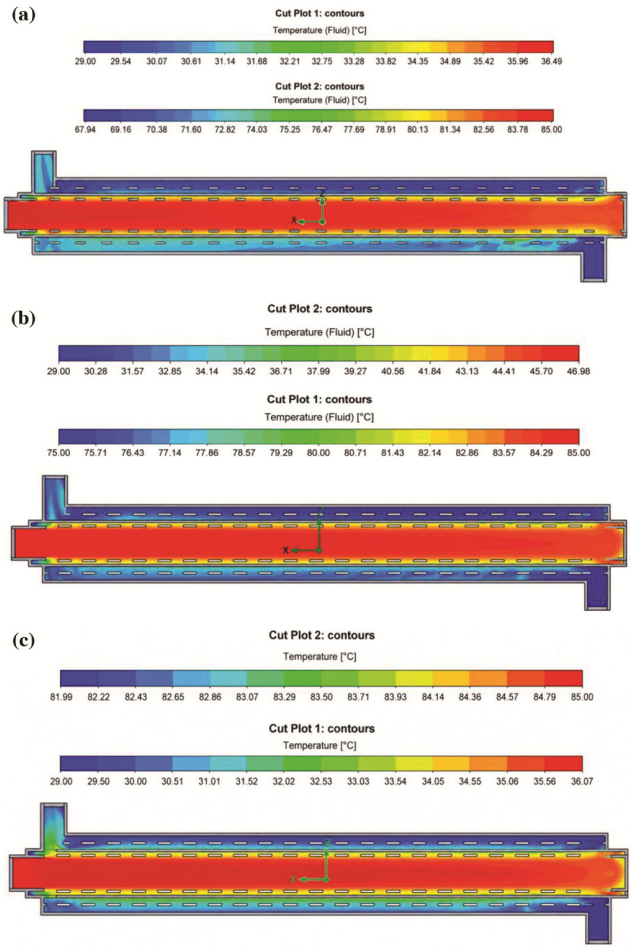

Fig. 8 — (a) Temperature Distribution in the Heat Exchanger with 8 mm pitch, (b) Temperature distribution in the heat exchanger with 10 mm pitch, (c) Temperature distribution in the heat exchanger with 12 mm pitch

413.5 W, and the corresponding CFD prediction was 420.2 W with only deviation of 1.6% which confirms that both numerical and experimental results are good agreement with each other. Accordingly, an 8 mm pitch has a high-turbulence but also high-resistance configuration and does not show the best thermal–hydraulic balance in comparison with the 10 mm pitch.

CFD Analysis for 10 mm Pitch Configuration

The 10 mm pitch configuration CFD analysis shows a positive compromise between jet interaction, turbulence, and fluid mixing with hydraulic resistance as shown in Fig. 8(b). And the continuous transfer of temperature contours between the hot entering water at about 85°C and the cold entering water at about 29°C is all enhanced by the disturbance generated with a pitch of 10 mm which could improve both convective exchange while not presenting excessive losses in terms of momentum as it happened for an 8 mm pitch. Experimental heat-transfer rate was 963.7 W, compared to 978.5 W from CFD, with only a difference of 1.5%. It can be concluded that among configurations in the investigated range of pitches, the 10 mm pitch was shown to have the best thermal–hydraulic performance.

CFD Analysis for 12 mm Pitch Configuration

Due to larger spacing between the perforations, the jet interaction and fluid mixing are comparatively weaker in the CFD analysis of 12 mm pitch configuration as shown in Fig. 8(c). The temperature contours shown in the figure confirmed a consistent trend for heat transfer from hot fluid to cold fluid along the exchanger, however reduced interaction of jets is around that led to low turbulence and lesser limit layer agitation compared to 10 mm configuration. The higher pitch is beneficial for decreasing hydraulic resistance, but diminished mixing cancels out increases in the convective heat transfer coefficient. The experimental heat-transfer rate was 908.7 W and the CFD prediction was 922.1 W with a deviation of only 1.5%, which shows satisfactory agreement between numerical simulation results and experimental data.

Quantitative CFD Interpretation of Pitch Effect

The findings from the CFD ascertain that perforation pitch is a direct variable influencing jet interaction, turbulence generation and enhancement in flow mixing and hydraulic resistance. For the 8 mm pitch, due to closely spaced perforations stronger jet interaction and flow disturbance is created. This will promote turbulence and break its thermal boundary layer; however, it will also increase hydraulic resistance and pressure loss. The heat-transfer rate measured is 413.5 W, which is low values considering the stronger turbulence applied: in this respect it seems that an excessive disturbance of the flow does not lead to a corresponding increase of heat-transfer enhancement.

From the CFD perspective, the temperature distribution of 10 mm pitch may be regarded as a uniform thermal field. The hot-stream temperature decreases from 85°C to about 83°C, while cold-stream temperature increases from 29°C to approximately 32.5°C The flow field results indicate strong interaction between fluid layers without any region of large stagnation or recirculation. This suggests good jet entrainment and boundary-layer disruption with low enough hydraulic disturbance. The corresponding experimental heat-transfer rate is 963.7 W, which holds the highest value from the other two configurations of cooling test conducted in this thesis.

In the case of 12 mm pitch, the larger distance decreases the number of jets as well as decreases their interaction. The CFD results demonstrate more laminar flow, less mixing zones, and lower turbulence intensity. The resulting temperature of the hot-stream decreases only from 85°C to about 84°C and the cold-stream temperature increases to about 32.3°C, and less interaction of jets was observed thus equivalent weaker boundary-layer disruption with thicker thermal boundary layer, which eventually decreases convective heat transfer. The larger pitch reduces flow resistance and pressure drop at the same time.

Hence, the CFD contours present a pitch-mandated compromise: 8 mm leads to effective turbulence and mixing but excessive hydraulic resistance, 12 mm alleviates hydraulic resistance but weakens jet interaction and thermal mixing and 10 mm provides the most balanced flow and temperature fields. This flow matches well with the measured heat-transfer rates of 413.5, 963.7, and 908.7 W for pitch of 8, 10 and 12 mm respectively;

Conclusions

The combined experimental and CFD investigation clearly shows that perforation pitch is a key geometric determinant of thermal-hydraulic performance in the context of counter-flow tubular minijet heat

exchangers. Comparisons between numerical solutions and experimental measurements reveal reasonably good agreement, with relative discrepancies of ±2–5% confirming that the present method can be used to quantify the flow and heat-transfer characteristics of these configurations. Among the three pitches close to corrected Reynolds number: 8 mm, 10 mm and 12 mm, the configuration of 8 mm generated high turbulence instead but also exhibited a difficulty by presenting high flow resistance leading to a heat-transfer rate only at 413.5 W whilst due to the reduction in flow resistance but loss in terms of jet interaction and mixing results were obtained at higher heat-transfer rates 908.7 W for configurations with 12mm respectively; Output User The 10 mm perforation pitch resulted in the best thermal-hydraulic performance, with a maximum heat-transfer rate of 963.7 W, an effectiveness value of 0.0625, and a cold-side outlet temperature near ~32.5°C; while maintaining a reasonable energy balance between the hot side and cold side. From an engineering view, the results indicate that reducing perforation pitch does not always guarantee better overall heat-exchanger performance because excessive jet interaction leads to increased hydraulic resistance, whereas high pitch reduces turbulence and heat-transfer enhancement. Hence, 10 mm pitch represents a practical compromise between the required mixing flow, turbulence generation, heat transfer and pressure-loss penalty for the explored range. This result offers a valuable design direction for compact tubular minijet exchangers subjected to augmented thermal rates while ensuring hydraulic losses do not exceed reasonable levels.

References

1 Akram M N, Liu Z, Zhang B and Li W, Numerical and experimental study of jet chamber designs for enhancing convective heat transfer in mini-tube heat exchangers, *Case Stud Therm Eng*, **78** (2026) 107702, doi: 10.1016/j.csite.2026.107702.

2 Hwary A, Miskdjian I, Gamea O & Abohadima S, Numerical analysis of heat transfer and turbulent flow friction in a tube equipped with perforated double conical rings, *J Eng Appl Sci*, **72(1)** (2025) 194, doi: 10.1186/s44147-025-00765-y.

3 Waware S Y, Ahire P P, Ghutepatil P R, Biradar R, Kadam A A, Kore S, Kurhade A S & Ghunake K B, Enhancing heat transfer in tubular heat exchanger using minijet technology, *J Mines Met Fuels*, **73(6)** 2025 1699–1706, doi: 10.18311/jmmf/2025/49028.

4 Waware S Y, Bote M A, Biradar R, Ahire P P, Kadam A A, Patil S P, Ghunake K B, Kore S & Kurhade A S, Experimental investigation of heat transfer improvement using perforated helical twisted tapes in a tube-in-tube heat exchanger, *J Mines Met Fuels*, **73(7)** (2025) 2083–2093, doi: 10.18311/jmmf/2025/49032.

5 Hsu C, Sayed B T, Rodrigues P, Mohammed H, Pushparajesh V, Vashisht A, Dash B, Shah S K, Hanoon T M & Obaida D S, Thermo-hydraulic performance analysis of a horizontal slinky-type geothermal heat exchanger under turbulent flow vonditions, *Sci Rep*, **16(1)** (2026) 16825, doi: 10.1038/s41598-026-43253-w.

6 Laue L K, Hattel J H & Abolmaali A M, CFD investigation of thermo-hydraulic performance enhancement in a double-pipe heat exchanger using non-uniformly spaced perforated ring inserts, *Energy Convers Manag*, **355** (2026) 121293, doi: 10.1016/j.enconman.2026.121293.

7 Rahman M A, Experimental investigations on single-phase heat transfer enhancement in an air-to-water heat exchanger with rectangular perforated flow deflector baffle plate, *Int J Thermodyn*, **26(4)** (2023) 31–39, doi: 10.5541/ijot.1285385.

8 Waware S Y, Kore S & Patil S P, Heat transfer enhancement in tubular heat exchanger with jet impingement: A review, *J Adv Res Fluid Mech Therm Sci*, **101(2)** (2023) 8–25, doi: 10.37934/arfmts.101.2.825.

9 Waware S Y, Kore S, Kurhade A S & Patil S P, Innovative heat transfer enhancement in tubular heat exchanger: An experimental investigation with minijet impingement, *J Adv Res Fluid Mech Therm Sci*, **116(2)** 2024 51–58, doi: 10.37934/arfmts.116.2.5158.

10 Alpha N A, Aondover I H & Kuhe A, Experimental and numerical studies of the effect of perforation configuration on heat transfer enhancement of pin fins heat sink , *Heat Transf*, **53(5)** (2024) 2525–2555, doi: 10.1002/htj.23051.

11 Chauhan G, Bisht V S, Bhandari P, Singh S, Shukla R, Ranakoti L & Bist A S, Numerical investigation of heat transfer enhancement in a double pipe heat exchanger using tangential perforated ring turbulators, *Arch Thermodyn*, **177** (2025), doi: 10.24425/ather.2025 .154191.

12 Saini S S, Tomar P, Kumar A, Dwivedi G & Kale S, Numerical investigation of heat transfer enhancement and flow performance of a tubular heat exchanger with surface modifications, *Heat Transf*, **54(8)** 2025 4989–5002, doi: 10.1002/htj.70041.

13 Abdulrasool A A, Aljibory M W, Abbas A K & Al-Silbi M M, A computational study of perforated helical tube inserted in a double pipe heat exchanger with fluid injection, *Int J Heat Technol*, **41(1)** (2023) 35–45, doi: 10.18280/ijht.410104.

14 Mahmoud M Sh, Abbas A & Abbas N Y, The role of perforated pin fins in forced convection for heat dissipation systems, *Heat Transf*, **55(4)** (2026) 2490–2505, doi: 10.1002/htj.70206.

15 Najim F T, Heat transfer enhancement inside a duct using turbulators, vortex generators, and baffles, *Khwarizmi*, (2024) 39–44, doi: 10.70470/khwarizmia/ 2024/006.

16 Louahdi M, Salhi J, Essaouini H, Zarrouk T & Lahlaouti M L, Three-dimensional analysis for optimizing thermo-hydrodynamic performance of heat exchangers with perforated semi-circular inserts, *Case*

Stud Therm Eng, **60** (2024) 104611, doi: 10.1016/j.csite.2024.104611.

17 Erdoğan B, Taşkaya G & Akbaba H, Experimental investigation of heat transfer and friction factor in laminar, transition and turbulence region for water flow in mini-micro channels, *Sci Rep*, **16** (2026), doi: 10.1038/s41598-026-56763-4

18 Kaithari D K, Siraskar G D, Biradar R, Kandharkar S, Kondhalkar G E, Kota P N, Kurhade A S & Waware S Y, Turbulence modelling and flow analysis of a trapped vortex combustor, *J Sci Ind Res*, **84(11)** (2025) 1241–1253, doi: 10.56042/jsir.v84i11.21774.

19 Kapade T T, Shah S K, Shah D S, Kumar N S, Bhor J K, Panwar V S & Singh G, Thermal analysis of v-cut twisted tape fitted heat exchanger: A numerical approach, *Int J Interact Des Manuf*, **19(3)** (2025) 1895–1911, doi: 10.1007/s12008-024-01883-2.

20 Jadhav P H, Sandhya V, Reddy V J, Reddy G S, Gnanasekaran N & Harsur S, Thermal performance evaluation and entropy generation analysis of partially filled aluminum metal foam heat exchanger, *Int J Heat Fluid Flow*, **117** (2026) 110109, doi: 10.1016/j.ijheatfluidflow.2025.110109.

21 Malwe P D, Mukayanamath A, Panchal H, Gupta N K, Prakash C & Abdul Zahra M M, Heat transfer enhancement of heat exchanger using rectangular channel with cavities, *Kerntechnik*, **88(4)** (2023) 532–540, doi: 10.1515/kern-2023-0032.

22 Nalavade S P, Patange A D, Prabhune C L, Mulik S S & Shewale M S, *Development of 12 Channel Temperature Acquisition System for Heat Exchanger using MAX6675 and Arduino Interface*, Springer Nature, 2018, 119–125, doi: 10.1007/978-981-13-2697-4_13.

23 Patil P S & Dhande K K, Rib spacing effect on heat transfer and pressure loss in a rectangular channel with semicircular ribs, *J Eng Res*, **10(3)** (2022) 216–229, doi: 10.36909/jer.10795.